



Science Arts & Métiers (SAM)

is an open access repository that collects the work of Arts et Métiers Institute of Technology researchers and makes it freely available over the web where possible.

This is an author-deposited version published in: <https://sam.ensam.eu>
Handle ID: <http://hdl.handle.net/10985/21220>

To cite this version :

Simone Vincenzo SURACI, Davide FABIANI, Xavier COLIN, Sébastien ROLAND - Multi scale aging assessment of low-voltage cables subjected to radio-chemical aging: Towards an electrical diagnostic technique - Polymer Testing - Vol. 103, p.107352 - 2021

Any correspondence concerning this service should be sent to the repository

Administrator : scienceouverte@ensam.eu





Science Arts & Métiers (SAM)

is an open access repository that collects the work of Arts et Métiers Institute of Technology researchers and makes it freely available over the web where possible.

This is an author-deposited version published in: <https://sam.ensam.eu>
Handle ID: <http://hdl.handle.net/null>

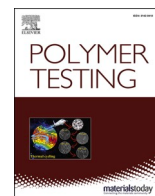
To cite this version :

Simone Vincenzo SURACI, Davide FABIANI, Sébastien ROLAND, Xavier COLIN - Multi scale aging assessment of low-voltage cables subjected to radio-chemical aging: Towards an electrical diagnostic technique - Polymer Testing - Vol. 103, p.107352 - 2021

Any correspondence concerning this service should be sent to the repository

Administrator : archiveouverte@ensam.eu





Multi scale aging assessment of low-voltage cables subjected to radio-chemical aging: Towards an electrical diagnostic technique

Simone Vincenzo Suraci^{a,*}, Davide Fabiani^a, Sébastien Roland^b, Xavier Colin^b

^a LIMES – DEI University of Bologna, Bologna (BO), Italy

^b PIMM, Arts et Métiers Institute of Technology, CNRS, CNAM, HESAM, Paris, France

ARTICLE INFO

Keywords:

Polymer aging
XLPE
Condition monitoring
Radiation aging
Ester index
dielectric spectroscopy
Antioxidants

ABSTRACT

In this article, the aging behavior of nuclear-grade low voltage cables, characterized by different geometries and insulation compositions, is investigated. Cables were subjected to radio-chemical aging at different dose rates (7 Gy/h, 66 Gy/h and 400 Gy/h), in order to simulate typical aging environments inside nuclear plants. The changes of insulation properties due to aging are investigated at different scales, aiming at highlighting possible correlations between molecular-scale properties and global macroscopic material behavior (e.g., mechanical and electrical ones). Microscale material behavior is investigated by means of FTIR spectroscopy and oxidation induction time (OIT) measurements, in order to evaluate material composition changes and material resistance to oxidation, respectively. On the other side, mechanical and electrical macroscopic properties are examined through tensile stress and dielectric spectroscopy measurements. It is found that aging is deeply influenced by the effect of additives (e.g. antioxidants) inside the insulation. In particular, the presence of antioxidants delays oxidation process allowing material modifications during the early aging states to be evaluated. Dielectric spectroscopy is demonstrated to properly follow all the stages of the degradation process, confirming its appropriateness as a non-destructive condition monitoring technique for cables. Finally, the evolution with aging of the dielectric response is associated with the variations of the considered chemical and mechanical properties, allowing the derivation of correlation master curves.

1. introduction

The use of polymeric materials as insulators for electrical cables is nowadays a consolidated technology [1–3]. in the electric plants. The considerable number of polymer types allows to select the one whose characteristics best fit the desired application. In particular, one of the most important discriminant properties to be considered is the cable rated voltage. From this, one can distinguish polymers for high, medium, and low voltage (HV, MV and LV, respectively) cable systems. Insulation materials for HV and MV cables are usually characterized by a high purity aiming at ensuring good operational performances even at high electrical fields. In point of fact, additives and fillers are demonstrated to possibly act as trapping centers of accumulated charges, causing electrical field distortions, whose effect can lead to cable failure in the case of high electrical fields [4–6].

Nonetheless, since modern cables are designed to guarantee a long service life, additives, mainly antioxidants, are needed inside the polymeric compound in order to prevent or slow down degradation

mechanisms occurring during the cable lifetime, e.g., oxidation [7–15].

On the other hand, inside low-voltage (LV) cable systems, electric fields are so low that impurities do not compromise reliability of these cables. Hence, it is possible to fill the base polymer with various types of additives (e.g., plasticizers, antioxidants, flame retardants) according to the application requirements. In LV cables additive concentration is estimated to be ~60% w/w in the polymeric compound, reducing the effective insulating performance of the resulting material [16,17]. Thus, it is evident, and already reported [12,18–21], that additives in such high amount can have an impact on both the physical-chemical and, consequently, on the electrical properties of both unaged material and on its behavior with aging.

In the case of LV cables for nuclear applications, one of the most common insulating compounds is the silane cross-linked polyethylene (Si-XLPE). Its wide application is given by the combination of its excellent electrical insulation properties with its low cost and easy manufacturing process. Si-XLPE is generally filled with both flame retardants and antioxidants. The former ones are intended to act as

* Corresponding author.

E-mail address: simone.suraci@unibo.it (S.V. Suraci).

<https://doi.org/10.1016/j.polymeresting.2021.107352>

Received 21 May 2021; Received in revised form 3 September 2021; Accepted 19 September 2021

Available online 2 October 2021

0142-9418/© 2021 The Authors.

Published by Elsevier Ltd.

This is an open access article under the CC BY-NC-ND license

(<http://creativecommons.org/licenses/by-nc-nd/4.0/>).

possible smoke suppressant in case of high temperatures (e.g. during a fire accident) and they usually reach $\sim 40\%$ w/w in typical NPP cables. The latter ones, in concentrations up to 2–3% w/w, permit the reaching of significantly long service lifetimes, often between 40 and 60 years [12–15].

The most common criterion for the evaluation of the health status of LV cable insulation systems, at least for those which are located in nuclear environment, is based on mechanical measurements, mainly the elongation-at-break (EaB) [17,22]. The advantage of using EaB lays on its proved and effective correlation with aging, which also permits the comparison of the results obtained with different stress levels [17].

In order to investigate the evolution of the material properties in a reasonable time, usually accelerated aging is used. This process aims at speeding up the normal aging processes through aggravated conditions of humidity, heat and, in the case of nuclear plants, radiations [10, 23–25]. Empirical and mathematical models, able to correlate accelerated test results with aging in real operation conditions, have been already developed using, e.g., EaB [23,26–29]. When ageing mechanisms are well identified, non-empirical kinetic models can also be developed to predict the material lifetime based on a structural embrittlement criterion [30–32]. However, tensile tests encounter some limitations. Firstly, they are destructive local measurements so that they may not be representative of the entire cable systems under test. Moreover, they are not always easy to perform due to the possible difficulties in reaching some parts of the cables, usually the most stressed ones.

In recent years, much research [17,23,33] has been focusing on the definition of an “ideal” and innovative condition monitoring technique for LV cables which shall be non-destructive, performed *in situ*, thus providing a simple end-of-life criterion for the considered cable.

Among the various techniques, dielectric spectroscopy recently gained more and more importance in the extruded cable research field. As a matter of fact, this technique meets most of the described requirements. It is non-destructive, it is capable to assess the health of the entire cable system and it has shown to have monotonic variation of the measured property [34–43]. Unfortunately, up to date, it lacks in enough knowledge to allow this technique to be fully operational for industrial applications.

Nonetheless, if the analyzed polymer is used as insulating material for cables, electrical properties are the ones to focus on, in order to avoid any unexpected cable crisis and breakdown. For this reason, correlating the change of electrical properties with physical-chemical properties, which are commonly used for the assessment of polymeric materials, can be crucial to verify the suitability of electrical techniques for the evaluation of the aging state of the insulating material. Furthermore, the proposed correlations raise the possibility to upgrade the actual monitoring techniques for cable diagnostics without losing the expertise obtained over several years of application of these approaches (e.g. predictive and life modelling methods).

That being said, this article aims at providing a wide and comprehensive view of physical, chemical and electrical properties of nuclear-scale LV cables subjected to radio-chemical aging. Investigated cables are characterized by different geometries and polymeric compounds, in order to highlight the impact of these characteristics on the resulting insulation properties. Finally, results coming from physical-chemical tests are correlated with the electrical response obtained through nondestructive dielectric spectroscopy measurements. This in order to evaluate the capability of this technique to follow the aging development throughout all the aging phases (e.g., antioxidant conversion and oxidation). In particular, the correlation of the electrical quantity with EaB is a key feature to succeed into the proposal of the dielectric spectroscopy as an efficient condition monitoring technique for LV nuclear cables, due to the broad use of the mechanical technique for cable aging assessment. This work is part of the European Project H2020 TeaM Cables, which aims at providing nuclear power plant operators with a novel methodology for nuclear LV cables maintenance through, among

others, developing a new multiscale modelling approach, to study polymer radiation aging.

2. Materials and methods

2.1. Cable specimens

Cables with different geometry and insulating compounds are studied in this article. The considered cable structures, namely coaxial and twisted pair, are reported in Fig. 1.

Primary insulation is based on the same silane crosslinked PE matrix (Si-XLPE), a widely used PE-based insulation for LV cables due to its easy processability and reduced costs. The PE lattice has been integrated with different kinds and quantities of additives. The detailed material compositions are reported in Table 1. Compound #1 applies to both coaxial and twisted pair cables (named twisted pair non filled cable), compound #2 applies to the twisted pair geometry only (twisted pair filled cable).

2.2. Accelerated aging

Cables were subjected to accelerated aging to replicate typical aging conditions inside nuclear environments. Three different dose rates were chosen to age cable specimens, namely: high, medium, and low dose rate corresponding to 400 Gy/h, 60 Gy/h, and 7 Gy/h respectively. Radio-chemical aging was performed in the Panoza (Medium and Low dose rate) and Roza (High Dose Rate) facility at UJV Rez, Czech Republic, through a ^{60}Co γ -ray source. Aging properties and durations are summarized in Table 2.

2.3. Dielectric spectroscopy results

Dielectric spectroscopy measurements were performed by means of the Novocontrol Alpha Dielectric Analyzer v2.2. The equipment was set using the following test parameters:

- Applied voltage: 3 V_{rms}
- Frequency range: 10^{-2} – 10^6 Hz
- Temperature: 50 °C (in oven).

This setup allows the investigation of the complex permittivity and $\tan\delta$. In this article, in order to get rid of possible geometry-related measurement discrepancies, only $\tan\delta$ results are reported.

$\tan\delta$, known also as dissipation factor (DF), is defined by Refs. [44, 45]:

$$\tan\delta = \frac{\epsilon'' + \sigma/\omega}{\epsilon'} \quad (1)$$

where ϵ' is the real part of permittivity defined as the dielectric constant of the material, ϵ'' is the imaginary part of permittivity related to the dielectric losses of the material, ω is the angular frequency of the wave and σ is the DC conductivity of the material.

In the case of coaxial cable samples, input voltage was applied to the inner conductor through a BNC plug and output signal was obtained through the copper wire braid shielding. For twisted pair cables, the input voltage was supplied to one of the two conductors while the output signal was detected from the other one, short-circuited with the copper braid shielding.

Among the frequencies in the analyzed region, it has been chosen to report data at a fixed frequency, namely 100 kHz (related to the dipolar polarization). This frequency was shown in the literature [35–37] to be associated with the increase of the aging products over time, mainly oxidized polymer chains, which have a strong dipolar behavior.

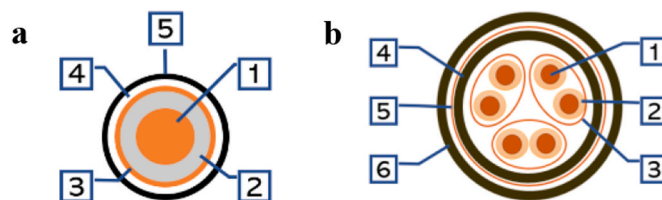


Fig. 1. (a) Multilayer structure of coaxial cables under investigation. (1) Conductor – Copper, (2) Primary insulation – XLPE, (3) Polymeric film – PET, (4) Shielding – Copper wire braid, (5) Sheath – Low smoke zero halogen rubber
(b) Multilayer structure of twisted pair cable under investigation. (1) Conductor – Copper, (2) Primary insulation, (3) Shielding – Copper wire braid, (4) Sheath, (5) External shielding – Copper wire braid, (6) External sheath.

Table 1
Specification of the insulating compounds. (phr – per hundred resin).

Compound #1 (coaxial and twisted pair cables)		
Component	Name	Concentration
Polymer matrix	Si-XLPE	–
Primary antioxidant	Irganox ® 1076	1 phr
Secondary antioxidant	Irganox ® PS802	1 phr
Compound #2 (twisted pair cables)		
Component	Name	Concentration
Polymer matrix	Si-XLPE	–
Primary antioxidant	Irganox ® 1076	1 phr
Secondary antioxidant	Irganox ® PS802	1 phr
Flame retardants	ATH	50 phr

Table 2
Accelerated aging conditions.

Aging type	Aging properties			
	Dose rate (Gy/h)	Sampling time (h)	Total absorbed dose (kGy)	Temperature (°C)
Low	7	3456	120	47
Medium	66	864	286	47
High	400	167	334	21

2.4. Oxidation induction time (OIT) measurements

OIT measurements are widely reported in the literature to be suitable for a quantitative investigation of antioxidant concentration inside the polymer sample [46].

OIT were measured at 210 °C with a TA instrument DSC Q10 calorimeter. XLPE samples with a mass between 5 and 10 mg were inserted inside the instrumentation furnace in an open aluminium pan. First heating run from room temperature to 210 °C was performed with a heating rate of 10 °C.min⁻¹ under a pure N₂ flow (50 mL min⁻¹); then, the temperature equilibrium was set at 210 °C for 5 min and finally, the gas was switched from N₂ to O₂ for an isotherm at 210 °C. Under pure oxygen, the test was stopped once an exothermal peak, referred to the induction of the oxidation, was registered. The time range between the switching of the furnace atmosphere and the onset of the exothermal peak (graphically obtained through the tangent method) is defined as the OIT.

2.5. Fourier transform infrared (FTIR) measurements

FTIR spectra were recorded through a PerkinElmer FTIR Frontier spectrometer equipped with a diamond/ZnSe crystal in attenuated total reflectance (ATR) mode. Each spectrum is given by the average of 16

scans in the spectral range from 4000 to 650 cm⁻¹, with a resolution of 4 cm⁻¹.

In order to investigate the oxidation development occurring inside the polymer during aging, ester index values were calculated per each aging period. The considered ester index is defined by:

$$\text{Ester index} = \frac{A_{1733\text{cm}^{-1}}}{A_{1472\text{cm}^{-1}}} \quad (2)$$

where $A_{1733\text{cm}^{-1}}$ is the absorbance of the considered ester peak, and $A_{1472\text{cm}^{-1}}$ is the absorbance of CH₂ scissoring vibration of PE crystal phase at 1472 cm⁻¹, whose value is supposed not to change during aging (reference peak).

Each specimen was tested at least three times in order to keep in account the possible inhomogeneous distribution of additives and the presence of locally aged spots.

2.6. Tensile stress tests

Tubular specimens of the minimal total length L of 60 mm were prepared after transversal cutting the insulated wire samples to pieces with length of about 65 mm.

For tensile tests, a calibrated Instron 3366 machine equipped with pneumatic grips with smooth steel surfaces was used. Specimens were placed between the two gauges and the following test parameters were applied:

- Testing (cross-head) speed: 50 mm/min
- Initial grip distance for specimens: 30 mm
- Rate of tensile test data acquisition: 1 data/s

The test is considered as completed when the breaking of the sample occurs [47].

As a result, the stress/strain curve is registered and obtained, from this it is possible to calculate the ultimate elongation value (Elongation-at-break) through the following equation:

$$\text{EaB}(\%) = \frac{(l - l_0)}{l_0} \cdot 100 \quad (3)$$

where l_0 and l are the initial and breaking useful lengths of the specimen, respectively.

3. Experimental results

3.1. Dielectric spectroscopy results

Fig. 2 reports the trend of dielectric losses ($\tan\delta$) at 100 kHz as a function of aging time for all the analyzed conditions and compounds.

In all cases, aging causes the growth of dielectric losses. One can

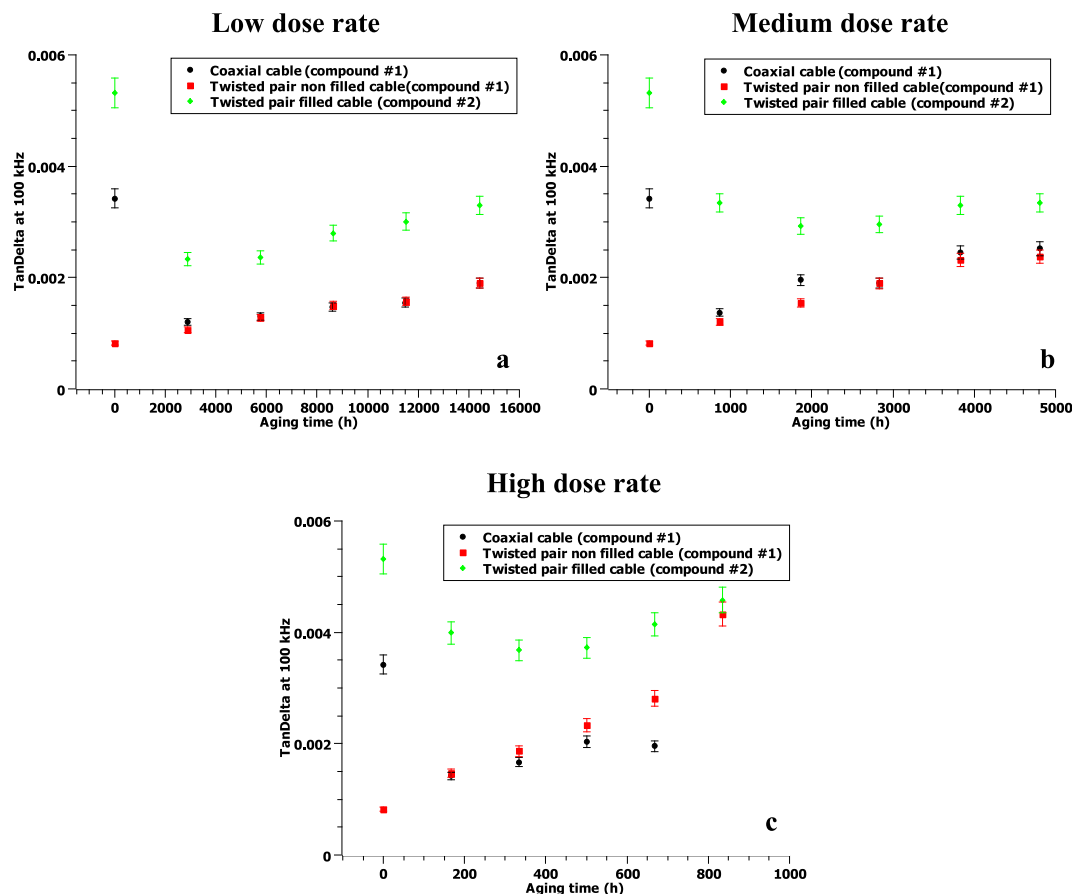


Fig. 2. Dielectric losses at 100 kHz as a function of aging time for the three aging conditions considered. (a) Low dose rate (7 Gy/h), (b) Medium dose rate (66 Gy/h), (c) High dose rate (400 Gy/h).

notice that the various aging severities reveal a different increasing trend of $\tan\delta$. In particular, harsher aging stresses cause a faster increase of the considered property. As an example, for coaxial cable, a $\tan\delta$ value $\sim 1.7 \cdot 10^{-3}$ is reached after $\sim 15\,000$ h in the case of low dose rate, $\sim 3\,000$ h in the case of medium dose rate and at ~ 200 h for the high dose rate. All this being said, there is a correspondence between $\tan\delta$ and degradation state of the polymer, indicating the suitability of dielectric spectroscopy as aging assessment technique for cables.

It is worth noting that $\tan\delta$ values do not monotonically increase starting from the initial state of the polymer (virgin sample). It has been highlighted in our previous works [35] that during the first aging period, different microstructural modification inside the polymer (e.g. antioxidant arising to the surface and possible degassing processes) can occur. As a result, $\tan\delta$ values are initially lowered due to the reduction of dipolar species, as it will be presented in the discussion section. However, these phenomena are not related to the aging state of the polymer, hence they could be considered as an initial stabilization of the insulating material.

Focusing on material compounds, it is worth highlighting that the two cable geometries characterized by compound #1 show comparable $\tan\delta$ values throughout the aging process, exception given for the highest dose rate of the coaxial cable. Here, the increase of the dielectric losses during the last aging period is almost negligible probably due to diffusion limited oxidation (DLO) phenomena [48,49] occurring inside the material. This phenomenon leads to an inhomogeneous oxidation throughout the polymer thickness. Indeed, the presence of particularly severe aging stressors brings to the formation of an external oxygen-proof layer, so that environmental oxygen cannot reach the inner part of the polymer. As a result, polymer does not significantly modify its bulk dipolar properties, as in the case here analyzed. Another

difference can be found in the unaged values of $\tan\delta$, which is larger for the coaxial cable (Fig. 2). Such behavior could be associated with the different starting additive concentration in the polymer matrix, as it will be presented in the following. Focusing on compound #2, the implementation of ATH inorganic fillers brings to a significant variation of the dielectric loss trend. These particles, as dipolar species, enhance the high frequency dielectric response. Consequently, the $\tan\delta$ trend is shifted upwards throughout the aging process with respect to the compound #1 response.

Fig. 3 exhibits the trend of the oxidation induction time (OIT) for the different aging conditions and cable geometries considered. Among the various available data from different compounds, it would be possible to outline a common behavior. In particular, during the first aging period, one can notice an abrupt decrease of the OIT value, followed by a slower but continuous decay of the property. Finally, OIT reaches a non-null value (around 2 min) which corresponds to the lowest value recordable through the tangent method used for the definition of OIT. Hence, it would be possible to claim that oxidation may have started even if OIT is not equal to zero.

With respect to the insulation compounds, coaxial cable owns the highest initial OIT value, suggesting a larger concentration of antioxidants, among the tested cables. This confirms the higher values of $\tan\delta$ found on unaged coaxial cables, see Fig. 2. Contextually, mid-term OIT are kept to higher values during aging, despite the similar decreasing trend. On the contrary, compound #2 shows the lowest starting OIT. The reason for that could be found in the introduction of ATH particles which could bring to ineffective morphological displacement of additives (e.g., antioxidants). According to Refs. [50,51], phenolic antioxidants could be deactivated by physical adsorption on the surface of e.g., carbon black by means of hydrogen bonding (i.e., through its OH groups). Thus,

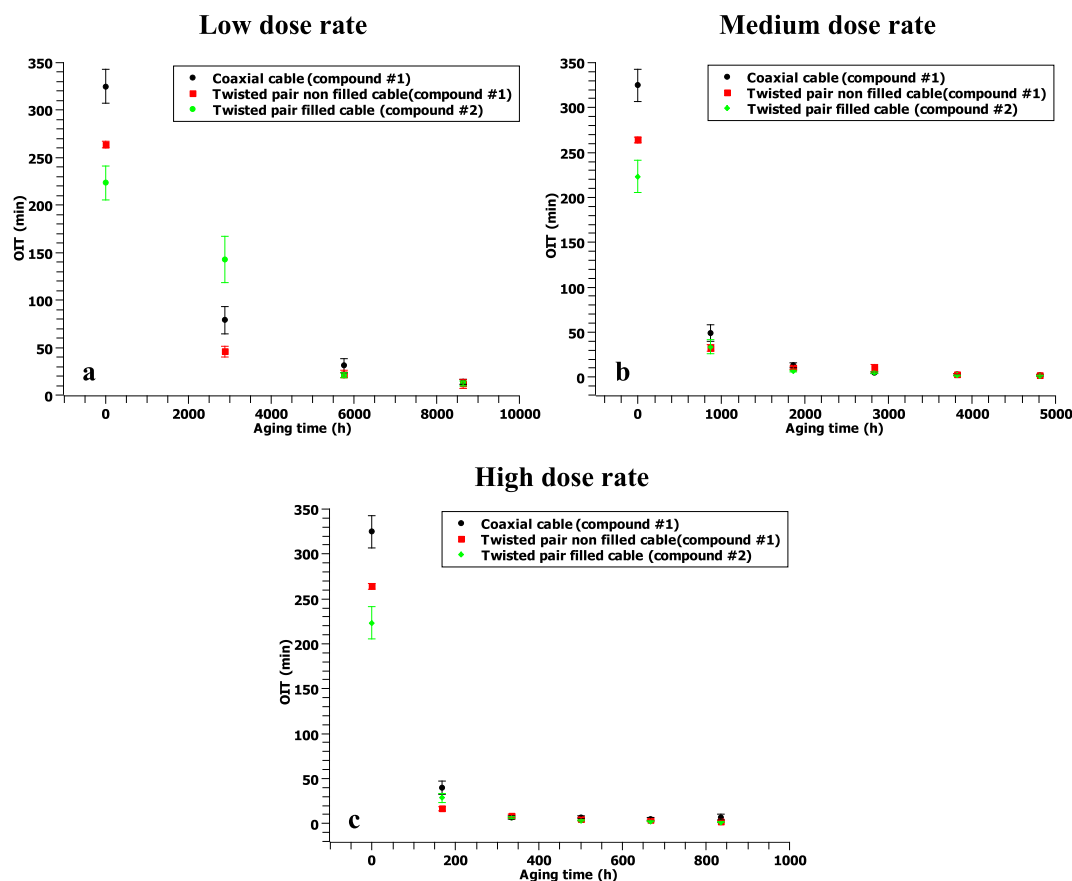


Fig. 3. Oxidation induction time values for the three different aging conditions considered. (a) Low dose rate (7 Gy/h), (b) Medium dose rate (66 Gy/h), (c) High dose rate (400 Gy/h).

it can be assumed that the antioxidants inside the considered polymeric compound could experience the same phenomenon due to the copious presence of OH groups in the tri-hydrated alumina (ATH). As a result, the stabilization reactions and the diffusion of antioxidant inside the amorphous phase may be significantly hindered, leading to a less effective protection against oxidation and lower OIT value (Fig. 3).

3.2. FTIR spectroscopy

FTIR spectroscopy tests were performed in ATR mode on the cables under study. Aiming at studying the oxidation evolution during the polymer aging and due to the huge number of data collected, only the ester index values are here reported. It is known that the major part of oxidized polymer chains is characterized by the presence of an ester bond [12,32,35,52]. For this reason, the ester index, whose calculation is reported in Section II.E, is commonly used as a first efficient approach to follow the degradation processes inside polyolefins.

Fig. 4 displays the trend of the ester index as a function of aging time for the three different cables and aging conditions considered. In particular, only the ester index values related to the surface of the materials are shown. Indeed, FTIR-ATR results coming from the polymer bulk showed to remain almost constant with aging. As known, oxidation reactions mainly occur on the material surface due to the presence of environmental oxygen. Possibly, the aging experienced by the cable specimens was not sufficient to completely oxidize the samples, leading to a limited oxidation in the polymer bulk and a non-variation of the index in the bulk of the material [12,35].

The ester index values related to the unaged material samples are significantly different one from the other. It is worth recalling at this point that the phenol antioxidants are characterized by an ester bond

whose stretching can be associated to the FTIR absorbance peak used for the calculation of the ester index [12,14,15]. Hence, the different ester indices related to the unaged samples can be linked to inhomogeneous dispersion of additives and, more generally, to the manufacturing process. A further confirmation of that could be found in the fact that the two twisted pair cables show similar trending behavior with aging, despite their different chemical compound. Indeed, due to the chemical formula of ATH ($\text{Al}_2(\text{OH})_3$), it can be said that these fillers have no impact on the ester peak, leaving the ester index response only related to products of antioxidants and oxidation.

Nonetheless, among the different ester index trends, it is possible to highlight a common behavior. In most cases, the parameter depicts an initial decrease followed by a stabilization and a final increase with aging.

The durations of the described phases are strictly linked to the severity of the aging conditions. In particular, the harsher the aging environment, the shorter the duration of the two initial phases, as expected. However, in the case of aging at high dose rate of the coaxial cable, the initial decrease is not present probably due to the strong aging conditions the cable is subject to.

3.3. Elongation-at-break

Fig. 5 displays the trend of the elongation-at-break for the three cables under test. In some cases (e.g., coaxial cable aged under low dose rate conditions), it was not possible to remove the inner conductor from the insulation without damaging the polymer due to the advanced degradation state. Hence, mechanical tests were not performed for those cables.

In all the conditions considered, the elongation-at-break values

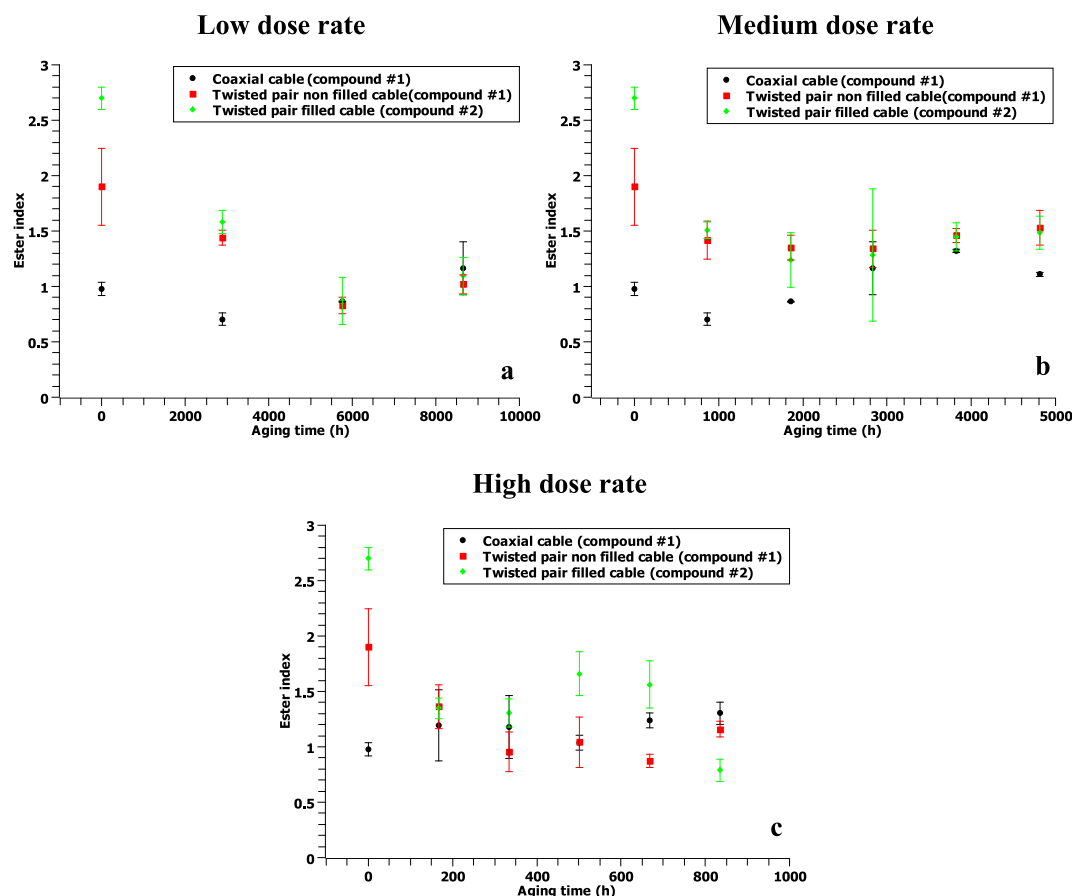


Fig. 4. Ester index as a function of aging time for the three different cables considered. (a) Low dose rate (7 Gy/h), (b) Medium dose rate (66 Gy/h), (c) High dose rate (400 Gy/h).

decrease with aging time, as expected. The decreasing trend can be considered almost linear with aging, suggesting a gradual and continuous degradation of the polymer throughout the aging time. Nonetheless, the harshness of aging affects the mechanical response of the material over time. In fact, despite the similar trend, the time needed to cause the same mechanical degradation is very different. As an example, the halving of the initial EaB value is reached slightly after ~ 800 h in the case of high dose rate while it is not reached even after $\sim 10,000$ h under low dose rate conditions, for the twisted pair filled cable.

Regarding the different insulation geometries, also in this case, it can be highlighted that same insulating material show similar trends with aging. Again, one can notice that the twisted pair non filled cable exhibits the highest value of initial EaB. The reason for that could be again possibly found in the manufacturing process and the displacement of additives, which modify the mechanical performance of the material. As a result, the EaB trend of the twisted pair non-filled cable, despite following the same decreasing law, is slightly shifted upwards in comparison to the one related to the coaxial cable.

The introduction of inorganic fillers results into a significant lowering of the initial EaB value (almost 50% of the initial value of compound #1). Therefore, due to the lower initial value, the decay of the property reaches the lowest recorded values among the different materials. A possible explanation for that will be presented in the next section.

4. Discussion

Ionizing radiations deposit a significant amount of energy inside the irradiated polymer. This energy is usually orders of magnitude higher than the mean chemical bond strength [53–56], so that radiation aging

is considered one of the most degradative aging conditions for organic compounds. Briefly reporting, the processes undertaken during radio-chemical aging can be divided into three stages. Firstly, the energy gained by the material (physical stage) brings to the creation of a significant number of activated molecules inside the polymeric matrix. In the following phase (physical-chemical stage), the excited molecules transfer energy to other molecules through collisions and chemical reactions. Consequently, new excited atoms and radicals are created. These radicals finally reach the chemical equilibrium (chemical stage) when they react with environmental oxygen, causing oxidation, or with themselves, giving birth to non-reactive species.

Most common oxidation processes have been described in literature for various kinds of plastics [11,52]. Main effects of oxidation process can be summarized in the decomposition of alkoxy radicals resulting into chain scission and the creation of new oxidation products i.e., carbonyl groups and alcohols.

However, oxidation process cannot be undertaken as long as antioxidant molecules are present. In particular, it could occur that antioxidant molecules are wrongly displaced in the polymer bulk or their concentration is higher than the one actually soluble inside the considered polymeric matrix. It has been demonstrated by Xu et al. [12] that if this occurs, antioxidant molecules tend to move towards the polymer surface by the mean of diffusion phenomena. Here, they exude on the sample surface where they rearrange into crystals.

Hence, in a tentative causal chain of oxidation degradation phenomena occurring inside the polymer, the first step can be considered as a sort of stabilization phase during which undissolved antioxidants are abruptly consumed during the first aging period due to both chemical reactions and physical loss.

During the following phase, antioxidant molecules react with

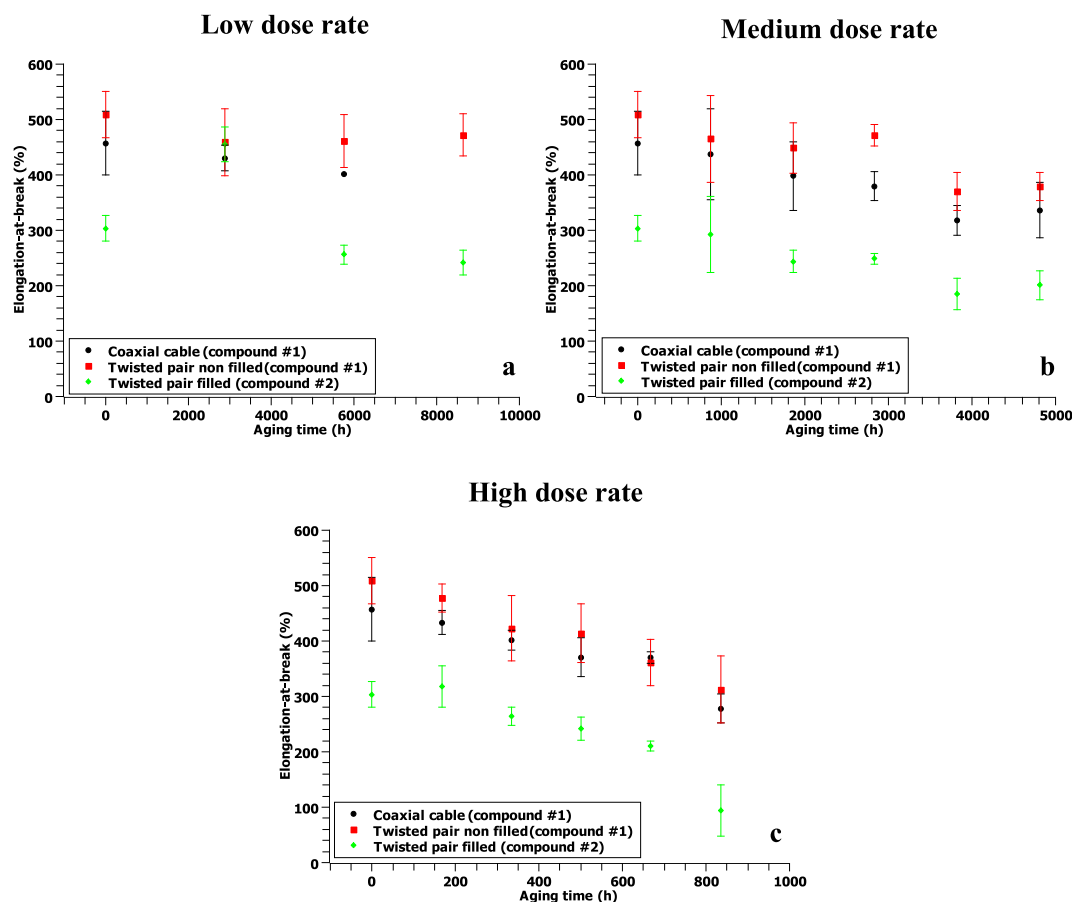


Fig. 5. Elongation-at-break as a function of aging time for the three different cables considered. (a) Low dose rate (7 Gy/h), (b) Medium dose rate (66 Gy/h), (c) High dose rate (400 Gy/h).

environmental oxygen to prevent or slow down oxidation process, giving rise to antioxidant degradation products, which are non-reactive polar species. Finally, after the running out of antioxidants, oxygen is free to bond with polymer chains and the above-described oxidation reactions can take place.

It has been found that the antioxidant degradation products exhibit the same ester bond of the antioxidant molecules. Hence, it would be difficult to separate the contribution of these two species through FTIR measurements, due to possible compensation of concentration of the ester bonds leading to the flattening of the ester index trend with aging (Fig. 4). However, being OIT measurements a quantitative technique for antioxidant concentration, the decrement of this factor during aging can be associated with the continuous consumption of antioxidant molecules.

The combination of these two testing techniques would allow a better understanding of the antioxidant degradation kinetics and it would permit the definition of the boundaries of the different aging phases. As an example, in all the studied cases, the ester index (Fig. 4) on the surface of the material shows a significant decrease during the first aging periods, possibly caused by the reduction of ester bond concentration of the antioxidant molecules. Similarly, the OIT values show an abrupt decrease, claiming a significant consumption of antioxidants inside the polymer matrix and checking the strictly correlation existing between these two quantities.

It is worth recalling at this point that both antioxidant molecules and degradation products are dipolar species. These species are characterized by non-zero dipolar momentum. As an example, the investigated antioxidant exhibits a dipolar momentum equal to ~ 4.8 D, while the value for an oxidized polymer chain (ketone) is about 3 D. Finally, the ATH fillers depict lower dipolar momentum value (~ 0.8 D) but, because

of their high concentration, they can significantly influence the dielectric spectrum as shown in Fig. 2. The correspondence between the concentration of antioxidant molecules and the electrical properties is also confirmed by the $\tan\delta$ values (Fig. 2), which decrease during the first aging period, as antioxidant concentration does, due to the reduction of polymer dipolar properties.

That being said, it would be possible to summarize the investigated property behavior throughout the three proposed aging phases, as follows:

1. Initial consumption of antioxidants. In this phase surface antioxidants are abruptly consumed due to aging stresses. As a consequence, the ester index and the OIT values decrease on the surface. The loss of antioxidant molecules leads to the lowering of the global polarity of the polymer, causing the reduction of $\tan\delta$ values (Fig. 2).
2. Conversion of antioxidants into degradation products. In this phase, antioxidants are converted into degradation species. As reported, as both base and product molecules are characterized by the same ester bonds, no variation can be seen in the ester index, which is kept almost constant (Fig. 4). In this region, OIT values slightly vary, and they are close to the minimum recordable by the instrumentation (~ 2 min). Finally, $\tan\delta$ values increase thanks to the formation of new dipolar species in the polymer bulk.
3. Arising of oxidized polymer chains. After the running out of antioxidant (OIT ~ 0 min), aging catalyzes oxidation reactions leading to the arising of new oxidized species (e.g., oxidized polymer chains). As a result, both the ester index and $\tan\delta$ values increase.

Therefore, it is evident that $\tan\delta$ values obtained from dielectric spectroscopy should change in the different aging phases described

above, depending on the polarity of the chemical species that are consumed/generated. In the following, some of the most significant correlations between electrical and chemical quantities detected in the different aging phases, are reported and discussed.

4.1. Antioxidant consumption and conversion

It has been already discussed that the first aging phenomenon refers to the conversion of antioxidant molecules into degradation products. As reported, OIT measurements are quantitative investigation of the antioxidant concentration in the material bulk. The antioxidant depletion factor (ADF) links the variation of OIT values, namely the antioxidant concentration, with aging time. It is defined as:

$$ADF = \frac{OIT_0 - OIT}{OIT_0} \quad (4)$$

where OIT and OIT_0 are the respective values for the aged and unaged samples.

This factor is correlable with the increase of the $\tan\delta$ values with aging time, since both the values consider the contribution of antioxidant concentration changes. On the one hand, the dielectric spectroscopy at the considered frequency (10^5 Hz) may evaluate the presence of antioxidant molecules and the arising of new antioxidant degradation products, which are dipolar species. On the other side, as presented, the consumption of the antioxidant molecules, hence the changes in OIT and ADF are associated with the conversion of these species into antioxidant degradation products.

Fig. 6 reports the trend of the high frequency $\tan\delta$ as a function of ADF.

From the figure above, it is possible to notice that after an abrupt variation of ADF, caused by the sudden consumption of antioxidants during the first aging periods, most experimental data are placed in the region 0.7–1. In this area, an exponential regression line can be built, confirming a correspondence between the grade of conversion of antioxidants, hence the increase of antioxidant degradation products, with the raise of $\tan\delta$ values. Finally, the regression line tends asymptotically to 1, corresponding to the complete running out of antioxidants ($OIT = 0$ min).

Further aging does not impact the OIT and ADF values, but it causes the increase of $\tan\delta$ suggesting the arising of new dipolar species which are no more related to the antioxidant kinetics (e.g., oxidized polymer chains).

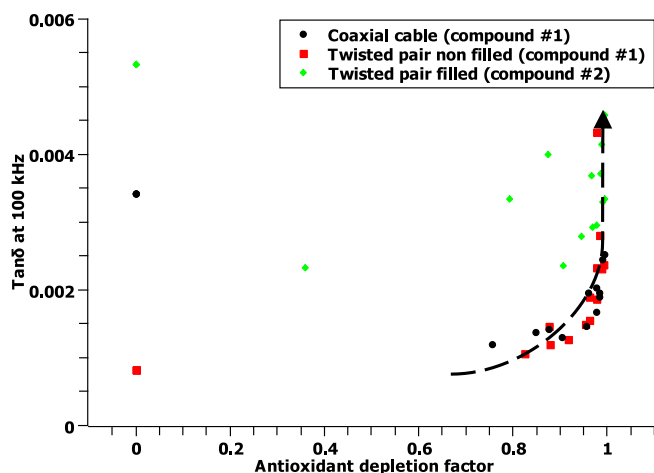


Fig. 6. High frequency dissipation factor as a function of the antioxidant depletion factor. Black and red data markers refer to materials without ATH. Green data markers refer to ATH-filled polymer. (For interpretation of the references to colour in this figure legend, the reader is referred to the Web version of this article.)

Focusing on the material compounds, one can observe that compound #1 (PE + AO) materials depict the same tendency, with similar dissipation factor and ADF values, despite the two different cable geometries.

The introduction of ATH fillers (compound #2) results into the shifting of the abovementioned trend upwards due to higher $\tan\delta$ values, as already discussed in Section III.A.

4.2. Arising of oxidized species

Once all the antioxidants are converted, hence $ADF = 100\%$, thermo-oxidative reactions can take place, leading to the creation of oxidized polymer chains. These molecules are highly dipolar species; hence they may respond under the effect of an external AC field, giving raise to $\tan\delta$ values. Moreover, they are characterized by an ester bond ($C=O$), whose presence may be evaluated through the FTIR spectroscopy.

Literature is plenty of studies [35,57] correlating the increase of the ester peaks with the aging time, suggesting the possibility to use the ester bands and their amplitude as an aging marker. These studies usually focus on neat highly pure polymers which are, in a certain sense, non-completely representative of the actual industrial application of the electrical insulating materials, in particular in low-voltage applications.

Indeed, in the case of industrial-scale polymers, the presence of additives (mainly antioxidants) can bring to an erroneous correlation between aging time and ester absorbance peak height. However, it has been reported in Section III.C that the last aging periods cause the increase of the ester index when OIT is almost equal to 0. This suggests that oxidation may have started and new esters, coming from the oxidation of polymeric chains, are created during aging. Contextually, the arising of these new species brings to the increase of the $\tan\delta$ value. Under these circumstances, it is possible to correlate the material response obtained through the dielectric spectroscopy and the ester index. Correlation plot is reported in Fig. 7.

In this graph, only the values referred to the third phase of aging are considered for the correlation, when the antioxidants have been already consumed, and oxidation reactions may take place inside the polymeric material. As it can be seen from Fig. 7, the correlation is quite evident, confirming the ability of dielectric spectroscopy at 100 kHz to follow the concentration of the oxidized polymer species, hence the degradation of the material. In particular, the proposed correlation is a key feature for the use of dielectric spectroscopy as an aging diagnostics technique, since it would be possible to relate the main degradation mechanism i.e., oxidation with the electrical quantity ($\tan\delta$), measurable on site.

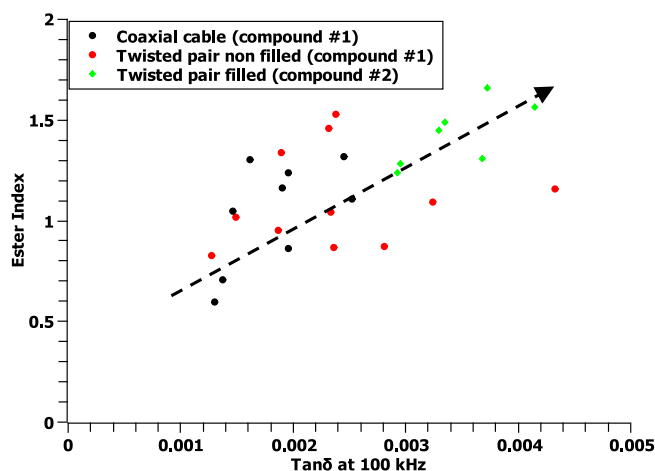


Fig. 7. High frequency dissipation factor versus ester index. Black and red data markers refer to materials without ATH. Green data markers refer to ATH-filled polymer. (For interpretation of the references to colour in this figure legend, the reader is referred to the Web version of this article.)

Even in this case, it is possible to divide the experimental data into two data clusters. Indeed, despite the data scattering given by the FTIR local analysis, compound #1 materials show similar values of ester index and $\tan\delta$. Finally, the introduction of ATH fillers brings to the shift of the data cluster towards higher $\tan\delta$ values (due to the presence of ATH polar species).

4.3. Correlation between mechanical and electrical properties

In Section III.D, it has been demonstrated that aging can cause the depletion of both mechanical and electrical properties of polymeric material. Under these circumstances, it would be possible to correlate these two sets of data. Correlation with EaB is significantly important since, as reported in the introduction, it represents the current state-of-the-art for cable aging assessment. In particular, the ultimate value of EaB used as end-of-life criterion is 50% of its absolute value. Resulting cross-plot is reported in Fig. 8.

Fig. 8 depicts a good correlation between the two properties. In particular, the decay of EaB values corresponds to the increase of the dielectric losses ($\tan\delta$) for all the analyzed conditions.

Also in the present case, it is possible to divide the trending behavior into two data clusters. The first one is related to the un-filled polymer (compound #1), where one can notice similar values between the two cable geometries. The second one is related to the presence of ATH fillers (compound #2). Here, experimental data are shifted towards a lower path of the same tendency line, giving raise to the second cluster. As already presented, ATH fillers are strongly dipolar species causing the increase of $\tan\delta$ values. On the other side, if they are present in conspicuous quantity, as in the case there considered, ATH fillers can regroup together because of the strong interactions between the OH groups present on their surface (hydrogen bonds). This agglomeration inside the polymer bulk brings to the reduction of the mechanical resistance, corresponding to lower EaB values. Microscopically, the ATH filler clusters can lead to a series of polymeric chain interruptions, reducing the elongation of the resulting polymer chain. In addition, ATH fillers are mineral-based compounds, hence their contribution to plastic elongation could be considered as negligible. As a result, macroscopically, the elongation at break significantly reduces for compound #2 materials.

As a further confirmation, Fig. 9 reports two X-ray tomography micrographs of the polymeric section of the un-filled (a) and filled (b) polymer. From this figure, it can be clearly seen that the unfilled material shows a homogenous pattern inside the polymer bulk. On the

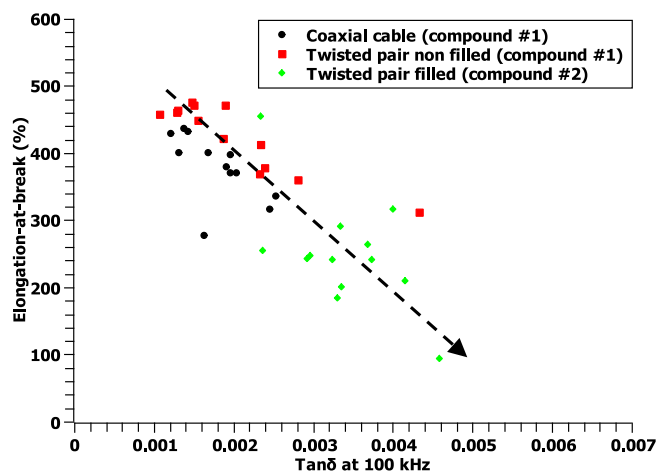


Fig. 8. Crossplot of EaB vs dissipation factor at 100 kHz. Black and red data markers refer to materials without ATH. Green data markers refer to ATH-filled polymer. (For interpretation of the references to colour in this figure legend, the reader is referred to the Web version of this article.)

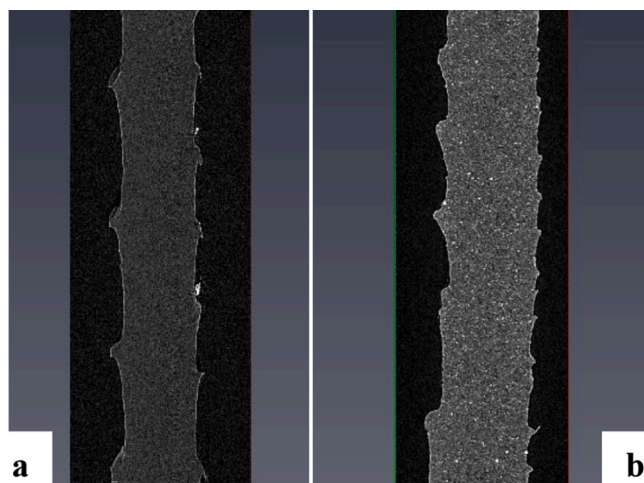


Fig. 9. Images from X-ray tomography of the cross-section of the unfilled (a) and filled (b) material. Courtesy of VTT Finland [58].

contrary, filled polymer section (Fig. 9b) exhibits the distribution of the ATH clusters in between the polymeric matrix.

Anyway, it is worth noting that no cable reached the end-of-life value of EaB for all the aging conditions analyzed. The lowest recorded value of EaB is equal to about 90% and it is related to the ultimate elongation of the highest dose of the harshest aging condition (high dose rate) for compound #2. Besides this, the proposed correlation seems to well fit the experimental data, raising the opportunity to upgrade the current state of the art of cable aging diagnostic, based on tensile tests, using electrical nondestructive tests.

5. conclusions

From the results shown in this article some conclusions can be drawn. First of all, cable geometry (coaxial/twisted pair) does not significantly affect insulation aging, as expected, but only the polymer initial composition. Then, the different physical-chemical (i.e., FTIR, OIT and tensile stress tests) and electrical (dielectric spectroscopy) techniques used to investigate cable aging exhibited good correlations. In particular, $\tan\delta$ at 100 kHz shows to coherently follow the variation of chemical and physical properties with aging.

However, the considered aging conditions showed to be not sufficiently harsh to cause significant degradation of both the analyzed compounds, since no substantial oxidation occurred inside the polymer. In particular, it has been shown that no cable reached the ultimate EaB required by the actual state of the art cable monitoring.

Nonetheless, such aging conditions allowed the investigation of the initial phases of the degradation process, which are mainly related to the presence of additives and fillers e.g., the antioxidant consumption and early degradation products formation. In particular, three different phases occurring during aging are presented: the initial consumption of antioxidants, their conversion into degradation products and, after the running out of antioxidants, the arising of new oxidized species. The introduction of inorganic fillers, e.g., flame retardants, showed not to have a significant impact on the degradation processes. However, they significantly influenced the mechanical and electrical behavior of the resulting polymer possibly due to the shortening of the polymer chain and filler dipolar properties, respectively.

That being said, the very little duration of the third phase (arising of oxidized products) confirmed that the variations in terms of mechanical, i.e., EaB and electrical properties, i.e., $\tan\delta$ are mainly related to microstructural modification inside the polymer, i.e., antioxidants consumption and chain rearrangements. Despite the limited oxidation process, it was possible to outline some correlations between the

different properties. As a result, dielectric spectroscopy has been successfully correlated with both mechanical and physical-chemical analyses, proving the suitability of this technique to follow the aging development throughout the three mentioned phases and assessing the possibility to use the dissipation factor ($\tan\delta$) as an aging marker for cable diagnostics.

Future work on this topic will include the development of a modelling approach aiming at evaluating the residual life of the analyzed cables in terms of mechanical endurance. Consequently, it would be possible to find a corresponding ultimate $\tan\delta$ value, i.e. a failure criterion for the cable in terms of the electrical property, upgrading the current state of the art of LV cable diagnostics. This could be a substantial step forward for the actual state of the art in cable diagnostics since it could be done *in situ* and in a non-destructive way.

Author statement

Simone Vincenzo Suraci, Conceptualization, Investigation, Formal analysis, Writing—original draft preparation. Davide Fabiani, Conceptualization, Formal analysis, Writing—review and editing, Supervision. Sébastien Roland, Conceptualization, Formal analysis. Xavier Colin, Conceptualization, Formal analysis, Writing—review and editing, Supervision.

Declaration of competing interest

The authors declare that they have no known competing financial interests or personal relationships that could have appeared to influence the work reported in this paper.

Acknowledgment

The project leading to this application has received funding from the Euratom research and training programme 2014–2018 under grant agreement No 755183. This publication reflects only the authors' view and the European Commission is not responsible for any use that may be made of the information it contains. Authors are grateful to UJV and VTT for performing tensile and X-ray tomography tests, respectively. The used tomography equipment was funded by the Academy of Finland through the RAMI infrastructure project (#293109).

References

- [1] W.F. Powers, The basics of power cable, *IEEE Trans. Ind. Appl.* 30 (3) (May 1994) 506–509, <https://doi.org/10.1109/28.293692>.
- [2] C. Zhou, H. Yi, X. Dong, Review of recent research towards power cable life cycle management, *High Volt.* 2 (3) (2017) 179–187, <https://doi.org/10.1049/hve.2017.0037>.
- [3] G. Mazzanti, et al., The insulation of HVDC extruded cable system joints. Part 1: review of materials, design and testing procedures, *IEEE Trans. Dielectr. Electr. Insul.* 26 (3) (Jun. 2019) 964–972, <https://doi.org/10.1109/TDEI.2019.007916>.
- [4] J. Castellon, S. Agnel, P. Notinger, Review of space charge measurements in high voltage DC extruded cables by the thermal step method, *IEEE Electr. Insul. Mag.* 33 (4) (Jul. 2017) 34–41, <https://doi.org/10.1109/MEI.2017.7956631>.
- [5] G. Rizzo, P. Romano, A. Imburgia, G. Ala, Review of the PEA method for space charge measurements on HVDC cables and mini-cables, *Energies* 12 (18) (Sep. 2019) 3512, <https://doi.org/10.3390/en12183512>.
- [6] M. Meunier, N. Quirke, A. Aslanides, Molecular modeling of electron traps in polymer insulators: chemical defects and impurities, *J. Chem. Phys.* 115 (6) (Aug. 2001) 2876–2881, <https://doi.org/10.1063/1.1385160>.
- [7] G. Singh, H. Bhunia, P.K. Bajpai, V. Choudhary, Thermal degradation and physical aging of linear low density polyethylene and poly(L-lactic acid) blends, *J. Polym. Eng.* 32 (1) (2012) 59–66, <https://doi.org/10.1515/polyeng-2011-0106>.
- [8] M. Sugimoto, A. Shimada, H. Kudoh, K. Tamura, T. Seguchi, Product analysis for polyethylene degradation by radiation and thermal ageing, *Radiat. Phys. Chem.* 82 (Jan. 2013) 69–73, <https://doi.org/10.1016/j.radphyschem.2012.08.009>.
- [9] J.I. Weon, Effects of thermal ageing on mechanical and thermal behaviors of linear low density polyethylene pipe, *Polym. Degrad. Stabil.* 95 (1) (Jan. 2010) 14–20, <https://doi.org/10.1016/j.polydegradstab.2009.10.016>.
- [10] M.C. Celina, Review of polymer oxidation and its relationship with materials performance and lifetime prediction, *Polym. Degrad. Stabil.* 98 (12) (Dec. 2013) 2419–2429, <https://doi.org/10.1016/j.polydegradstab.2013.06.024>.
- [11] E. Richaud, X. Colin, C. Monchy-Leroy, L. Audouin, J. Verdu, Polyethylene stabilization against thermal oxidation by a trimethylquinoleine oligomer, *Polym. Degrad. Stabil.* 94 (3) (Mar. 2009) 410–420, <https://doi.org/10.1016/j.polydegradstab.2008.11.018>.
- [12] A. Xu, S. Roland, X. Colin, Physico-chemical characterization of the blooming of Irganox 1076® antioxidant onto the surface of a silane-crosslinked polyethylene, *Polym. Degrad. Stabil.* 171 (Jan. 2020) 109046, <https://doi.org/10.1016/j.polydegradstab.2019.109046>.
- [13] A. Xu, S. Roland, X. Colin, Thermal ageing of a silane-crosslinked polyethylene stabilised with a thiodipropionate antioxidant, *Polym. Degrad. Stabil.* 181 (Nov. 2020) 109276, <https://doi.org/10.1016/j.polydegradstab.2020.109276>.
- [14] A. Xu, S. Roland, X. Colin, Physico-chemical analysis of a silane-grafted polyethylene stabilised with an excess of Irganox 1076®. Proposal of a microstructural model, *Polym. Degrad. Stabil.* 183 (Jan. 2021) 109453, <https://doi.org/10.1016/j.polydegradstab.2020.109453>.
- [15] A. Xu, S. Roland, X. Colin, Thermal ageing of a silane-crosslinked polyethylene stabilised with an excess of Irganox 1076®, *Polym. Degrad. Stabil.* (Apr. 2021) 109597, <https://doi.org/10.1016/j.polydegradstab.2021.109597>.
- [16] R.A. Assink, K.T. Gillen, R. Bernstein, Nuclear Energy Plant Optimization (NEPO) final report on aging and condition monitoring of low-voltage cable materials, SAND2005- 7331 (Nov. 2005) 875986, <https://doi.org/10.2172/875986>.
- [17] S.W. Glass, L.S. Fifield, G. Dib, J.R. Tedeschi, A.M. Jones, T.S. Hartman, State of the Art Assessment of NDE Techniques for Aging Cable Management in Nuclear Power Plants FY2015, Sep. 2015, <https://doi.org/10.2172/1242348>, PNNL-24649, M2LW-15OR0404024, 1242348.
- [18] S.V. Suraci, D. Fabiani, C. Li, Additive effect on dielectric spectra of crosslinked polyethylene (XLPE) used in nuclear power plants, in: 2019 IEEE Electrical Insulation Conference (EIC), 2019, pp. 410–413, <https://doi.org/10.1109/EIC43217.2019.9046600>.
- [19] S.V. Suraci, D. Fabiani, K. Sipilä, H. Joki, Filler impact analysis on aging of crosslinked polyethylene for nuclear applications through dielectric spectroscopy, in: 2019 IEEE Conference on Electrical Insulation and Dielectric Phenomena (CEIDP), Oct. 2019, pp. 166–169, <https://doi.org/10.1109/CEIDP47102.2019.9009787>.
- [20] H. Lim, S.W. Hoag, “Plasticizer effects on physical-mechanical properties of solvent cast Soluplus® films, *AAPS PharmSciTech* 14 (3) (Sep. 2013) 903–910, <https://doi.org/10.1208/s12249-013-9971-z>.
- [21] E. Planes, L. Chazeau, G. Vigier, J. Fournier, I. Stevenson-Royaud, Influence of fillers on mechanical properties of ATH filled EPDM during ageing by gamma irradiation, *Polym. Degrad. Stabil.* 95 (6) (Jun. 2010) 1029–1038, <https://doi.org/10.1016/j.polydegradstab.2010.03.008>.
- [22] Shuaishuai Liu, L.S. Fifield, N. Bowler, Towards aging mechanisms of cross-linked polyethylene (XLPE) cable insulation materials in nuclear power plants, in: 2016 IEEE Conference on Electrical Insulation and Dielectric Phenomena (CEIDP), Oct. 2016, pp. 935–938, <https://doi.org/10.1109/CEIDP.2016.7785636>.
- [23] K. Simmons, et al., Determining Remaining Useful Life of Aging Cables in Nuclear Power Plants – Interim Status for FY2014, Milestone Report M3LW-140R04022, 2014.
- [24] C. Blivet, J.F. Larché, Y. Israël, P.-O. Bussière, J.L. Gardette, Thermal oxidation of cross-linked PE and EPR used as insulation materials: multi-scale correlation over a wide range of temperatures, *Polym. Test.* 93 (Jan. 2021) 106913, <https://doi.org/10.1016/j.polymertesting.2020.106913>.
- [25] X. Chi, J. Li, M. Ji, W. Liu, S. Li, Thermal-oxidative aging effects on the dielectric properties of nuclear cable insulation, *Art. no. 10, Materials* 13 (Jan. 2020) 10, <https://doi.org/10.3390/ma13102215>.
- [26] International Atomic Energy Agency, IAEA-TECDOC-1188, Assessment and Management of Ageing of Major Nuclear Power Plant Components Important to Safety, vol. 1, 2000.
- [27] B. Pinel, F. Boudaud, A methodology to predict the life duration of polymers used in nuclear power stations. Industrial needs and their approach, *Nucl. Instrum. Methods Phys. Res. Sect. B Beam Interact. Mater. Atoms* 151 (1) (May 1999) 471–476, [https://doi.org/10.1016/S0168-583X\(99\)00134-2](https://doi.org/10.1016/S0168-583X(99)00134-2).
- [28] C. Monchy-Leroy, P. Therond, Nuclear cables and lifetime simulation, in: *Jicable Conference* 2007, 2007.
- [29] F. Espinosa, J.C. Gard, K. Bic, B. Poisson, Comparison of different methodologies to assess the lifetime of cable, in: *Jicable Conference* 2011, 2011.
- [30] N. Khelidj, X. Colin, L. Audouin, J. Verdu, A simplified approach for the lifetime prediction of PE in nuclear environments, *Nucl. Instrum. Methods Phys. Res. Sect. B Beam Interact. Mater. Atoms* 236 (1) (Jul. 2005) 88–94, <https://doi.org/10.1016/j.nimb.2005.03.259>.
- [31] X. Colin, C. Monchy-Leroy, L. Audouin, J. Verdu, Lifetime prediction of polyethylene in nuclear plants, *Nucl. Instrum. Methods Phys. Res. Sect. B Beam Interact. Mater. Atoms* 265 (1) (Dec. 2007) 251–255, <https://doi.org/10.1016/j.nimb.2007.08.086>.
- [32] S. Hettal, S. Roland, K. Sipilä, H. Joki, X. Colin, A new analytical model for predicting the radio-thermal oxidation kinetics and the lifetime of electric cable insulation in nuclear power plants. application to silane cross-linked polyethylene, *Polym. Degrad. Stabil.* 185 (Mar. 2021) 109492, <https://doi.org/10.1016/j.polydegradstab.2021.109492>.
- [33] F. Yu, Electrical Power Research Institute (EPRI), A review of nondestructive evaluation technologies for cable system integrity - report #3002000470 - Sections 3-4, EPRI - Technical report, 2013.
- [34] S.V. Suraci, D. Fabiani, J. Cohen, In situ defect recognition analysis on long cables through nondestructive reflectometry and dielectric spectroscopy methods: a comparison, in: 2020 IEEE Electrical Insulation Conference (EIC), 2020, pp. 41–44, <https://doi.org/10.1109/EIC47619.2020.9158583>.

- [35] S.V. Suraci, D. Fabiani, A. Xu, S. Roland, X. Colin, Ageing assessment of XLPE LV cables for nuclear applications through physico-chemical and electrical measurements, *IEEE Access* 8 (2020) 27086–27096, <https://doi.org/10.1109/ACCESS.2020.2970833>.
- [36] E. Linde, L. Verardi, D. Fabiani, U.W. Gedde, Dielectric spectroscopy as a condition monitoring technique for cable insulation based on crosslinked polyethylene, *Polym. Test.* 44 (Jul. 2015) 135–142, <https://doi.org/10.1016/j.polymertesting.2015.04.004>.
- [37] L. Verardi, D. Fabiani, G.C. Montanari, V. Pláček, Electrical aging markers for low-voltage cable insulation wiring of nuclear power plants, in: 2012 IEEE 10th International Conference on the Properties and Applications of Dielectric Materials, Jul. 2012, pp. 1–4, <https://doi.org/10.1109/ICPADM.2012.6318966>.
- [38] E. Linde, L. Verardi, P. Pourmand, D. Fabiani, and U. W. Gedde, "Non-destructive condition monitoring of aged ethylene-propylene copolymer cable insulation samples using dielectric spectroscopy and NMR spectroscopy," *Polym. Test.*, vol. 46, pp. 72–78, Sep. 2015, doi: 10.1016/j.polymertesting.2015.07.002.
- [39] R. Gagliani, N. Bowler, S. Glass, L. Fifield, Capacitance measurements for nondestructive testing of aged nuclear power plant cable, in: *Proceedings Of 47th Annual Review Of Progress In Quantitative Nondestructive Evaluation*, Portland (USA), 2019.
- [40] S.V. Suraci, D. Fabiani, L. Mazzocchetti, L. Giorgini, Degradation assessment of polyethylene-based material through electrical and chemical-physical analyses, *Energies* 13 (3) (Jan. 2020) 650, <https://doi.org/10.3390/en13030650>.
- [41] D. Fabiani, S.V. Suraci, Broadband dielectric spectroscopy: a viable technique for aging assessment of low-voltage cable insulation used in nuclear power plants, *Polymers* 13 (4) (2021) 494, <https://doi.org/10.3390/polym13040494>.
- [42] D. Fabiani, S.V. Suraci, S. Bulzaga, Aging investigation of low-voltage cable insulation used in nuclear power plants, in: 2018 IEEE Electrical Insulation Conference (EIC), Jun. 2018, pp. 516–519, <https://doi.org/10.1109/EIC.2018.8481139>.
- [43] R.S.A. Afia, M. Ehtasham, Z.Á. Tamus, Electrical and mechanical condition assessment of low voltage unshielded nuclear power cables under simultaneous thermal and mechanical stresses: application of non-destructive test techniques, *IEEE Access* 9 (2021) 4531–4541, <https://doi.org/10.1109/ACCESS.2020.3048189>.
- [44] J.W. Schultz, Dielectric spectroscopy in analysis of polymers, *Encyclopedia of Analytical Chemistry* (2006), <https://doi.org/10.1002/9780470027318.a2004>.
- [45] A.K. Jonscher, Dielectric relaxation in solids, *J. Phys. D Appl. Phys.* 32 (14) (Jan. 1999) R57–R70, <https://doi.org/10.1088/0022-3727/32/14/201>.
- [46] S. Liu, S.W. Veysey, L.S. Fifield, N. Bowler, Quantitative analysis of changes in antioxidant in crosslinked polyethylene (XLPE) cable insulation material exposed to heat and gamma radiation, *Polym. Degrad. Stabil.* 156 (Oct. 2018) 252–258, <https://doi.org/10.1016/j.polymdegradstab.2018.09.011>.
- [47] IEC Standard 60811 501:2012: "Electric and Optical Fibre Cables – Test Methods for Non Metallic Materials – Part 501: Mechanical Tests – Tests for Determining the Mechanical Properties of Insulating and Sheathing Compounds".
- [48] K.T. Gillen, R.L. Clough, Rigorous experimental confirmation of a theoretical model for diffusion-limited oxidation, *Polymer* 33 (20) (Jan. 1992) 4358–4365, [https://doi.org/10.1016/0032-3861\(92\)90280-A](https://doi.org/10.1016/0032-3861(92)90280-A).
- [49] C. Sinturel, N.C. Billingham, A theoretical model for diffusion-limited oxidation applied to oxidation profiles monitored by chemiluminescence in hydroxy-terminated polybutadiene, *Polym. Int.* 49 (9) (2000) 937–942, [https://doi.org/10.1002/1097-0126\(200009\)49:9<937::AID-PI399>3.0.CO;2-8](https://doi.org/10.1002/1097-0126(200009)49:9<937::AID-PI399>3.0.CO;2-8).
- [50] N.S. Allen, et al., Ageing and stabilisation of filled polymers: an overview, *Polym. Degrad. Stabil.* 61 (2) (Jan. 1998) 183–199, [https://doi.org/10.1016/S0141-3910\(97\)00114-6](https://doi.org/10.1016/S0141-3910(97)00114-6).
- [51] G. Scott, *Atmospheric Oxidation and Antioxidants*, Elsevier, 1993, <https://doi.org/10.1016/C2009-0-15759-8>.
- [52] Bruno Fayolle, E. Richaud, X. Colin, J. Verdu, Review: degradation-induced embrittlement in semi-crystalline polymers having their amorphous phase in rubbery state, *J. Mater. Sci.* 43 (22) (Nov. 2008) 6999–7012, <https://doi.org/10.1007/s10853-008-3005-3>.
- [53] E. Yousif, R. Haddad, Photodegradation and photostabilization of polymers, especially polystyrene: review, *Dec, SpringerPlus* 2 (1) (2013) 398, <https://doi.org/10.1186/2193-1801-2-398>.
- [54] G. Spadaro, Effect of irradiation temperature and dose rate on the mechanical tensile behaviour of low density polyethylene, *Eur. Polym. J.* 29 (9) (Sep. 1993) 1247–1249, [https://doi.org/10.1016/0014-3057\(93\)90156-A](https://doi.org/10.1016/0014-3057(93)90156-A).
- [55] S. Ilie, R. Senetscu, *Polymeric Materials Review on Oxidation, Stabilization and Evaluation Using CL and DSC Methods*, 2009. No. CERN-TE-Note-2009-004.
- [56] R.L. Clough, K.T. Gillen, G.M. Malone, J.S. Wallace, Color formation in irradiated polymers, *Radiat. Phys. Chem.* 48 (5) (Nov. 1996) 583–594, [https://doi.org/10.1016/0969-806X\(96\)00075-8](https://doi.org/10.1016/0969-806X(96)00075-8).
- [57] C. Rouillon, et al., Is carbonyl index a quantitative probe to monitor polypropylene photodegradation? *Polym. Degrad. Stabil.* 128 (Jun. 2016) 200–208, <https://doi.org/10.1016/j.polymdegradstab.2015.12.011>.
- [58] Konsta Sipilä, Jukka Kuva, XLPE insulators. Dataset - etsin.fairdata.fi, 2020, <https://doi.org/10.23729/7589d5c7-49b4-4c2c-bb4d-5466477bcc0f>.